Available online at www.sciencedirect.com
ScienceDirect
Trans. Nonferrous Met. Soc. China 21(2011) 2216−2224
Transactions of Nonferrous Metals Society of China
www.tnmsc.cn

Electrodeposition and corrosion behavior of nanostructured Ni-TiN composite films

ZHU Xu-bei[1], CAI Chao[2, 3], ZHENG Guo-qu[1], ZHANG Zhao[3], LI Jin-feng[4]

1. College of Chemical Engineering, Zhejiang University of Technology, Hangzhou 310014, China;
2. State Key Laboratory for Mechanical Behavior of Materials, Xi'an Jiaotong University, Xi'an 710049, China;
3. Department of Chemistry, Zhejiang University, Hangzhou 310027, China;
4. School of Materials Science and Engineering, Central South University, Changsha 410083, China

Received 11 October 2010; accepted 11 January 2011

Abstract: The Ni-TiN nanocomposite film was successfully electrodeposited on brass copper substrates. The microstructures of the Ni-TiN nanocomposite film were investigated using scanning electron microscopy (SEM) and transmission electron microscopy (TEM). Its average grain size was analyzed through X-ray diffraction (XRD), and its anti-corrosion property was studied through potentiodynamic scanning curves and electrochemical impedance spectroscopy (EIS). The results show that the morphology of Ni-TiN composite film is sensitively dependent on the electroplating current density, TiN nanoparticle concentration, solution stirring speed, bath temperature and pH value of solution. The average grain size of the optimized nanocomposite film is about 50 nm. Meanwhile, the Ni-TiN nanocomposite films are much more resistant to corrosion than pure Ni coatings.
Key words: Ni-TiN nanocomposite film; electrodeposition; electrochemical impedance spectroscopy

1 Introduction

The excellent properties of nanostructured composite film (NSCF) compared with traditional polycrystalline and amorphous materials make it a promising material for many industrial applications, especially for the micro devices [1−3]. Consequently, extensive research effort has been made on NSCF [4−7]. Compared with other techniques for NSCF synthesis, electroplating possesses many advantages including [8] low cost and industrial applicability, simple operation, versatility, high production rates, few size and shape limitations, and high probability of transferring the technology to existing electroplating and electroforming industries. Thereby, the electrodeposition technique has aroused attention of many investigators in the world.

Nickel, as a kind of engineering materials, is a widely used metal matrix. Nowadays, Ni-SiC composites have been commercialized for the protection of friction parts, combustion engines and casting moulds [9]. Literatures with regard to fabricating, mechanical properties and co-deposition mechanism of Ni-SiC nanocomposited films have been well-documented [3, 5, 9]. However, the co-deposition of nickel with other nanoparticles such as Si_3N_4, TiN and TiC, which are also good wearable materials and have similar configuration with SiC, has less been reported.

TiN nanoparticles have electrical and thermal conductivity, and good corrosion resistance. Therefore, TiN coatings on stainless steels have been processed as bipolar plates of polymer electrolyte membrane fuel cells [8−10]. Meanwhile, TiN possesses high hardness (microhardness of 21 GPa), and can be used as secondary phase to enhance strength and toughness of metal or ceramics substrate. Therefore, TiN nanoparticles would have a good prospect of application as an additive.

In this study, Ni-TiN nanocomposite film is prepared using traditional DC electroplating technique and characterized using SEM, TEM and XRD techniques. The influences of the solution agitation speed, TiN nanoparticle concentration, current density, bath pH value and bath temperature on the microstructure of

Foundation item: Projects (50771092, 21073162) supported by the National Natural Science Foundation of China; Project (2005DKA10400-Z15) supported by the Ministry of Science and Technology of China
Corresponding author: ZHANG Zhao; Tel: +86-571-85615190; E-mail: eaglezzy@zjuem.zju.edu.cn
DOI: 10.1016/S1003-6326(11)60998-9

electrodeposited Ni-TiN nanocomposite film are investigated. The anti-corrosion property of the Ni-TiN electrodeposited nanocomposite films is studied also.

2 Experimental

2.1 Preparation of Ni-TiN nanocomposite film

Brass copper (64Cu36Zn, hereinafter) rods embedded by Teflon with an exposure area of 0.50 cm^2 was used as the substrates. Before electroplating, the substrates were sequentially polished with silicon carbide emery papers through $400^{\#}$ to $800^{\#}$ followed with alumina paste of 2.5 μm, and rinsed with distilled water, washed with acetone, rinsed with double distilled water again, and then blow-dried by air. A double-electrode system with the substrate as the working electrode and a platinum foil as the counter electrode were employed for electroplating [10]. The electroplating solutions consisting of 0.38 mol/L $Ni_2SO_4·7H_2O$, 0.17 mol/L $NiCl_2$, 0.49 mol/L H_3BO_3, a few surfactant and a certain concentration of TiN particles were prepared using analytical grade reagents and double-distilled water. The electroplating process for every sample was operated for 10 min. Before electroplating, the electroplating solutions were stirred using ultrasonic for 24 h to ensure the good dispersion of TiN nanoparticles. TiN nanoparticles used in this study had an average diameter of less than 14 nm, of which the surface-to-volume ratio was 120 m^2/g, and the density was 0.08 g/cm^3. During the electroplating, the electroplating solution was agitated with different agitation speeds from 600 r/min to 1 200 r/min. Meanwhile, the solution temperature, pH value, TiN nanoparticles concentration and current density were also changed, as shown in Table 1. The electroplating DC current was provided by a transistor potentiostat (Model ZF−9, China), and a thermostat water tank was used to control the bath temperature.

Table 1 Electroplating parameters for Ni-TiN composite film

Parameter	Value
TiN concentration/($g·L^{-1}$)	2, 6, 8, 10
Agitation speed/($r·min^{-1}$)	600, 800, 1 000, 1 200
Current density/($A·dm^{-2}$)	0.2, 0.4, 0.5, 0.6, 0.8
Bath pH	2, 3, 4, 5
Bath temperature/°C	30, 40, 50, 60

The morphology of the obtained Ni-TiN composite film was observed on a scanning electron microscope (SEM, SIRION). The microstructure of the optimized nano-composite film was observed through a transmission electron microscope (TEM, JEOL200CX). Its average grain size was analyzed through a X-ray diffractometer (XRD, Iguacu D/max 2550PC) using Cu K_α radiation with the wavelength of 1.5418 Å and calculated by the Debye-Scherrer formula.

2.2 Corrosion characterization of Ni-TiN nanocomposite films

The potentiodynamic scanning curves and EIS of the pure Ni film and the Ni-TiN nanocomposite film, were measured in a three-electrode cell at room temperature ((25±0.5) °C). The electrodeposits were used as working electrodes, a large platinum foil acted as counter electrode, and a saturated calomel electrode (SCE) acted as reference electrode, respectively. All potentials were referred to SCE. The corrosion medium was 3.5% (mass fraction) NaCl solution prepared using AR grade reagents and double-distilled water.

After immersion of 1 h in NaCl solution, the EIS measurements were performed using a 283 potentiostat (VMP2, Princeton Applied Research, USA) at the open circuit potential (OCP) and carried out in the frequency range of 100 kHz−0.01 Hz. The applied sinusoidal signal amplitude was 5 mV. The potentiodynamic scanning curves in NaCl solution were obtained with a CHI 660A electrochemical workstation (CH Instruments Ins., US), and always initiated from OCP of −0.25 V in a positive direction.

3 Results and discussion

3.1 Influence of electroplating parameters on morphology of Ni-TiN composite films

MA et al [11] and NWOKO and SHREIR [12] and GUGLIELMI [13] reported that the microstructure of traditional composite films was mainly influenced by electroplating current density and particle concentration in the bath. Meanwhile, our previous work [14−15] also found that the agitation speed of solutions, bath pH value and bath temperature significantly influenced the microstructures of the electrodeposited composites. Consequently, the influence of the TiN nanoparticles concentration, current density, solution agitation speed, bath pH value and bath temperature were investigated in details.

3.1.1 Effect of TiN nanoparticles concentration

When the agitation speed, current density, bath temperature, bath pH value were kept as 900 r/min, 0.6 A/dm^2, (50±1) °C and pH 4, respectively, the influence of TiN nanoparticles on the composite film morphology is shown in Fig. 1. The structure of the composite film is refined with increasing the TiN concentration from 2 g/L to 8 g/L (Figs. 1(a)−(d)). However, as the TiN concentration in the electroplating bath is further increased to 10 g/L, this concentration is not advantageous

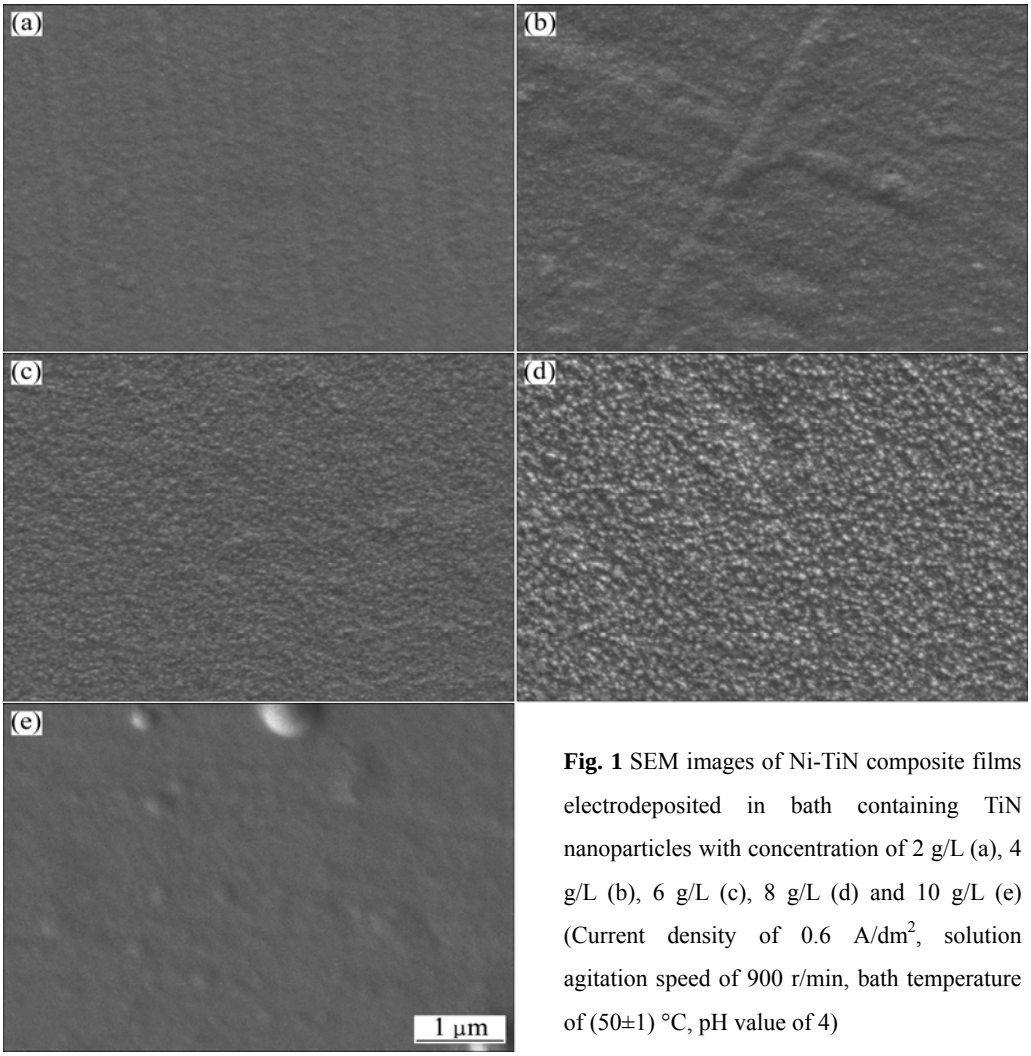

Fig. 1 SEM images of Ni-TiN composite films electrodeposited in bath containing TiN nanoparticles with concentration of 2 g/L (a), 4 g/L (b), 6 g/L (c), 8 g/L (d) and 10 g/L (e) (Current density of 0.6 A/dm^2, solution agitation speed of 900 r/min, bath temperature of (50±1) °C, pH value of 4)

for further grain refinement (Fig. 1(e)).

According to the theoretical model proposed by GUGLIELMI [13] for the traditional composite electroplating, the particles suspending in the electroplating bath come into electrodeposited composite film through two successive adsorption steps. In the first step, the particles are loosely adsorbed on the cathode surface, of which the content is in equilibrium with the suspension. In the second step, the particles are irreversibly adsorbed. It was reported that inert nanoparticles adsorbed on the cathode surface increased the cathodic polarization and inhibited the growth of metal crystallites simultaneously [11, 13]. Consequently, it is rational to deduce that higher TiN nanoparticle concentration in the solution should refine the structures of electrodeposited composite film, and also increase the TiN content. It was also known that further increasing the nanoparticle concentration accelerates both the agglomeration effect and the subsequent gravitational sedimentation of the particles [13]. As the concentration of TiN nanoparticles is further increased to 10 g/L, their agglomeration and subsequent gravitational sediment-tation result in the decrease in the TiN content in the electrodeposited composite film.

3.1.2 Effect of electroplating current density

The SEM images of the electrodeposited film at different current densities (D_k) are shown in Fig. 2. It is noted that the other electroplating parameters were fixed as follows, TiN concentration 8 g/L, solution agitation speed 900 r/min, bath temperature (50±1) °C, and pH 4. And the electric charge to the cathode at different current density was maintained constant by changing the electrodeposition time. As the current density is increased from 0.2 A/dm^2 to 0.4 A/dm^2, the grain is refined (Figs. 2(a), (b)). However, as the current density is further increased from 0.6 A/dm^2 to 0.8 A/dm^2, it is found that the grain is not further refined (Figs. 2(c) and (d)). This means that too much low current density (0.2 A/dm^2) or too much high current density (0.8 A/dm^2) is disadvantageous for electrodepositing nanocomposite.

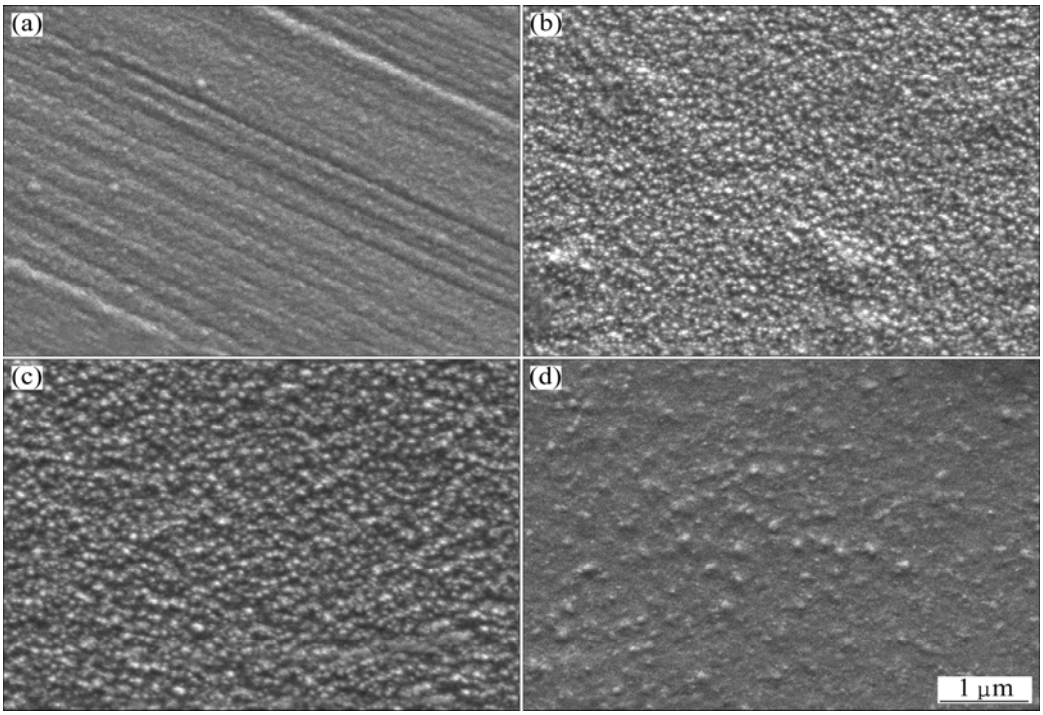

Fig. 2 SEM images of Ni-TiN composite films electrodeposited at current density of 0.2 A/dm^2 (a), 0.4 A/dm^2 (b), 0.6 A/dm^2 (c), 0.8 A/dm^2 (d) (TiN nanoparticle concentration: 8 g/L, solution agitation speed: 900 r/min, bath temperature: (50±1) °C, pH value: 4)

Based on our potentiometric titration [15], the surfaces of TiN nanoparticles are positively charged in the electroplating solution at pH 2.5–7. The TiN nanoparticles are surrounded by a thin layer of negatively charged species such as OH^- ions, especially by the anionic surfactant which is used to chemically modify TiN nanoparticles prior to their addition into the electroplating solution. These ions form ionic clouds around the TiN particles. Meanwhile, in the traditional composite electroplating process, there are three possible controlling factors for inert particles to be entrapped in metal matrix, i.e., exotic agitation, electrophoresis and adsorption. Here, the electrophoresis rate of the TiN nanoparticles is directly associated with the current density. Consequently, in the case of too low current density of 0.2 A/dm^2, the TiN nanoparticle should possess low electrophoresis rate, which will result in low TiN nanoparticle content in the electrodeposited film, and therefore favor the preferential growth of nickel crystallite (Fig. 2(a)).

On the other hand, according to the two-successive-adsorption-step mechanism proposed by GUGLIELMI et al [13], the first loose adsorption step is substantially physical but not electrochemical in character and it is less sensitive to current density than Ni^{2+} ions. Consequently, too high current density of 0.8 A/dm^2 accelerates the reduction processes and crystal growth of nickel. Therefore, it is not favorable for further grain refinement. Meanwhile, with increasing the current density, the hydrogen reduction rate is accelerated and therefore decreases the TiN content in the electrodeposited composite film, which also favors the crystal growth of nickel in the electrodeposited composite film. The results tally tightly with those obtained by WALTER et al [16].

3.1.3 Effect of solution agitation speed

The influence of solution agitation speed was studied when other electroplating parameters were fixed as follows: TiN concentration 8 g/L, current density 0.5 A/dm^2, bath temperature (50±1) °C, and pH 4. Figure 3 shows the SEM images of the electrodeposited film at various agitation speeds. When the agitation speed is increased from 600 r/min to 800 r/min, the film surface is more uniform. It seems that the grain is refined. However, when it is further increased from 1 000 r/min to 1 200 r/min, the TiN content in the composite film is decreased, and the grain does not be further refined.

In the case of low solution agitation speed (600 r/min), the amount of TiN nanoparticles adsorbed on cathode surface certainly decreases, due to lower exotic forced convection. Meanwhile, the agglomeration and gravitation effect of the particles is higher than the agitation effect. This causes the suspended TiN nanoparticles to agglomerate and subside, and also leads to their low adsorption amount on cathode surface. As the agitation speed is increased to 800 r/min and 1 000 r/min, their adsorption amount on cathode surface is increased, due to the higher exotic forced convection.

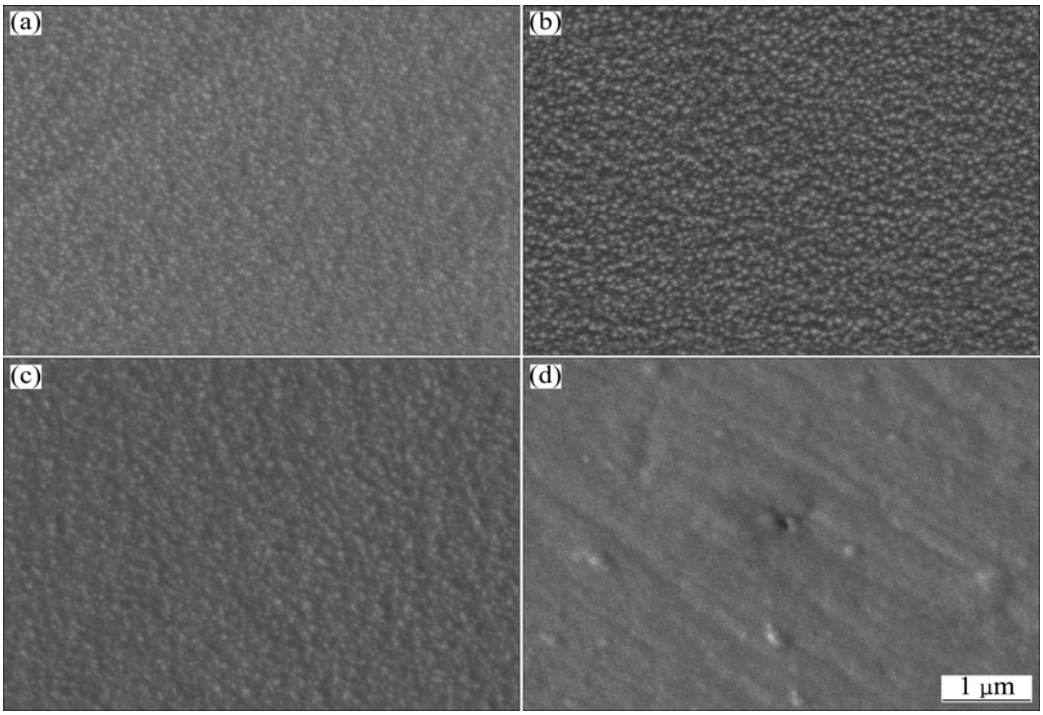

Fig. 3 SEM images of Ni-TiN composite films electrodeposited with agitation speed of 600 r/min (a), 800 r/min (b), 1 000 r/min (c) and 1 200 r/min (d) (TiN nanoparticle concentration: 8 g/L, current density: 0.5 A/dm^2, bath temperature: (50±1) °C, pH value: 4)

Therefore, the TiN nanoparticle content in the electrodeposited film is increased, which correspondingly increases the cathodic polarization and the spatial resistance for small nickel crystallites to grow. As a result, the electrodeposited composite film containing higher TiN content with nanostructure is formed. These results are consistent with those obtained by NOWAK et al [17], who found that the addition of SiC nanoparticles into nickel-electroplating bath remarkably increased the charge-transfer resistance of electroplating processes.

However, as the agitation speed is further increased to 1 200 r/min, according to the two-successive-adsorption-step mechanism proposed by GUGLIELMI [13], the intensive forced convection will bring away the loosely adsorbed TiN nanoparticles from the cathode surface, decreasing the TiN nanoparticle content in the electrodeposited film. Consequently, the absence of TiN nanoparticles leads to the nickel grain growth.

3.1.4 Effect of bath temperature

The influence of bath temperature was studied when the other electroplating parameters were fixed as follows: TiN concentration 8 g/L, current density 0.5 A/dm^2, solution agitation speed 800 r/min, and pH 4. Figure 4 shows the SEM images of the electrodeposited film at various temperatures. With the elevation of the bath temperature from 30 °C to 50 °C, the thermodynamic movement of molecules in the solution speeds up and the solution viscosity decreases, which increases the stability and dispersion of the electroplating bath. Meanwhile, the TiN nanoparticle migration rate also increases with increasing the bath temperature, resulting in higher TiN nanoparticle content in the electrodeposited film and finer grain size, as shown in Figs. 4 (a)−(c).

However, high bath temperature of 60 °C also decreases the interfacial tension between the electrodeposited composite and H_2 bubbles generated during electroplating, and accelerates the departing rate of H_2 bubbles from the cathode, accelerating the de-adsorption of TiN nanoparticles from the cathode surface and reducing their content in the electrodeposited film (Fig. 4(d)).

It is also found that as the bath temperature is elevated to higher than 70 °C, the stability of the electroplating bath is decreased due to rapid water evaporation, leading to difficult electroplating operation and deteriorating the electrodeposited film quality.

3.1.5 Effect of bath pH value

The influence of bath pH value was studied when the other electroplating parameters were fixed as follows: TiN concentration 8 g/L, current density 0.5 A/dm^2, solution agitation speed 800 r/min, and bath temperature (50±1) °C. Figure 5 shows that the SEM images of electrodeposited composite film at different pH values. In the case of pH 2, too many H_2 bubbles generate and depart from cathode during electroplating, which inhibits the adsorption of TiN nanoparticles on the cathode surface. Therefore, it seems that the TiN nanoparticle

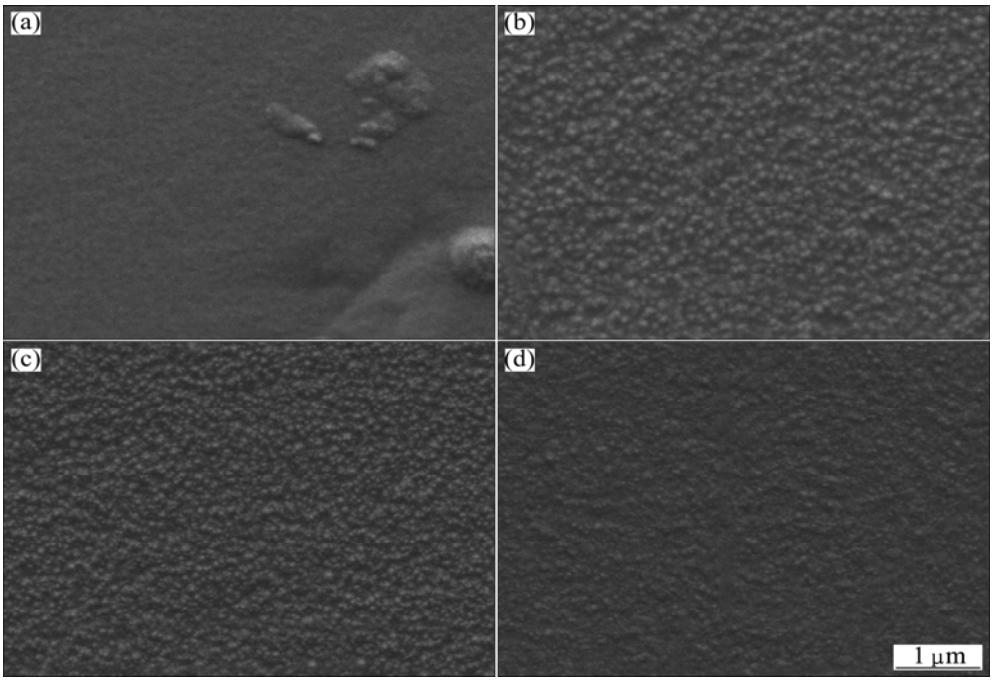

Fig. 4 SEM images of Ni-TiN composite films electrodeposited at temperature of 30 °C (a), 40 °C (b), 50 °C (c) and 60 °C (d) (TiN nanoparticle concentration: 8 g/L, current density: 0.5 A/dm^2, solution agitation speed: 800 r/min, pH value: 4)

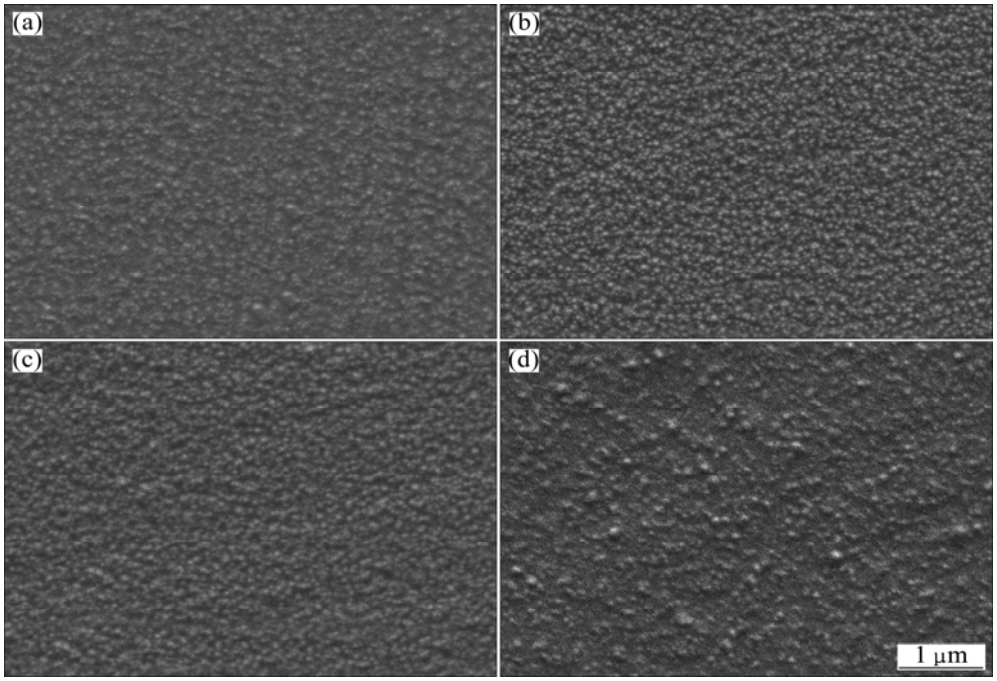

Fig. 5 SEM images of Ni-TiN composite films electrodeposited at pH value of 2 (a), 3 (b), 4 (c) and 5 (d) (TiN nanoparticle concentration: 8 g/L, current density: 5 A/dm^2, solution agitation speed: 800 r/min, bath temperature: (50±1) °C)

content of the composite film electrodeposited at pH 3−4 (Figs. 5(b) and (c)) is higher than that at pH 2 (Fig. 5(a)), and the grain is also finer. While, in the case of pH 5, the intermediates such as $Ni(OH)^+$ or $Ni(OH)^+$ (ads) are generated and adsorbed on the cathode surface during electroplating [18], which inhibits both the first loosely adsorbing processes of TiN nanoparticles and the nucleation rate of nickel crystals, therefore favors the crystal growth of nickel in the electrodeposited film (Fig. 5(d)).

3.2 Microstructure of optimized Ni-TiN nano-composite films

From the above experiments, the electroplating

conditions for Ni-TiN nanocomposite film are optimized as follows: 0.38 mol/L $Ni_2SO_4·7H_2O$, 0.17 mol/L $NiCl_2$, 0.49 mol/L H_3BO_3, 2.4 g/L surfactant, 8 g/L TiN nanoparticles, D_k = 0.5 A/dm^2, t=(50±1) °C, pH=3 and the solution agitation speed 800 r/min. The corresponding SEM image of the film is shown in Fig. 5(b). It is found that the nickel grain is very fine and uniform.

Figure 6 represents the XRD pattern of the optimized Ni-TiN nanocomposite film. Compared with the standard XRD pattern of pure Ni, the XRD peaks of Ni in this composite film are broadened, indicating a grain refinement. Based on this XRD pattern, the average size (g) of the electrodeposited film was estimated using following Debye-Scherre's equation:

$$g=k·\lambda/(\beta·\cos\theta)$$

where k is a constant taken to be 0.94; λ is the wave length of X-ray used (1.541 8 Å); β is the FWHM of the peak; and θ is Bragg's angle. Then, the average grain size was calculated to be about 50 nm.

The nanostructure of the electrodeposited Ni-TiN composite film was also proved by the bright-field TEM image (Fig. 7). Meanwhile, Fig. 7 also reveals that TiN nanoparticles are distributed uniformly in the electrodeposited film.

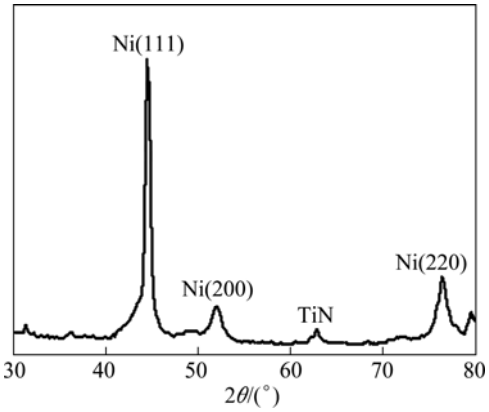

Fig. 6 XRD pattern of optimized Ni-TiN nanocomposite film

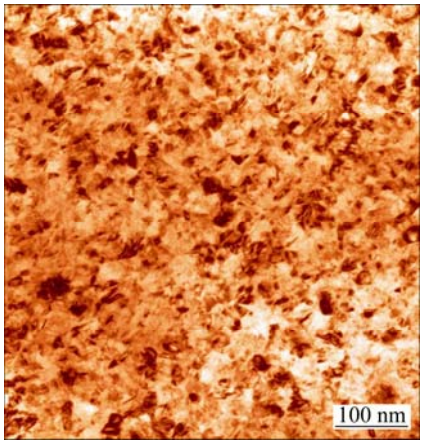

Fig. 7 Bright field TEM image of Ni-TiN nanocomposite film

3.3 Corrosion behavior of optimized Ni-TiN nanocomposite films

Figure 8 illustrates the EIS plots of the nanostructured Ni-TiN composite film and pure Ni coating immersed in neutral 3.5% NaCl solution for 1 h. The two EIS plots are similar. The time-constant number has been determined through the method developed by van der WEIJDE et al [19−20]. From the EIS diagrams (including Nyquist and Bode plots), it is found that each EIS plot contains two capacitive loops above the real axis. The capacitive loop at high frequency may be caused by the electrodeposited film, while the low frequency capacitive loop is correlated with the corrosion charge transfer resistance. Based on the above analysis, the EIS plots shown in Fig. 8 are analyzed using two time-constant electrochemical equivalent circuit (EEC) model (Fig. 9) and fitted through a Boukamp program. In Fig. 9, R_s is the electrolyte resistance, R_1 and R_t represent the resistances of Ni-TiN nanocomposite film and charge transfer resistance, respectively. While, CPE1 and CPE2 are the electrode surface capacitance (including deviation from ideal behavior) and the double-layer capacitance. The fitted parameters are shown in the Table 2.

The charge transfer resistance (R_t) can reveal the electrochemical corrosion rate. The smaller the R_t is, the larger the corrosion rate will be. From Table 2, it can be

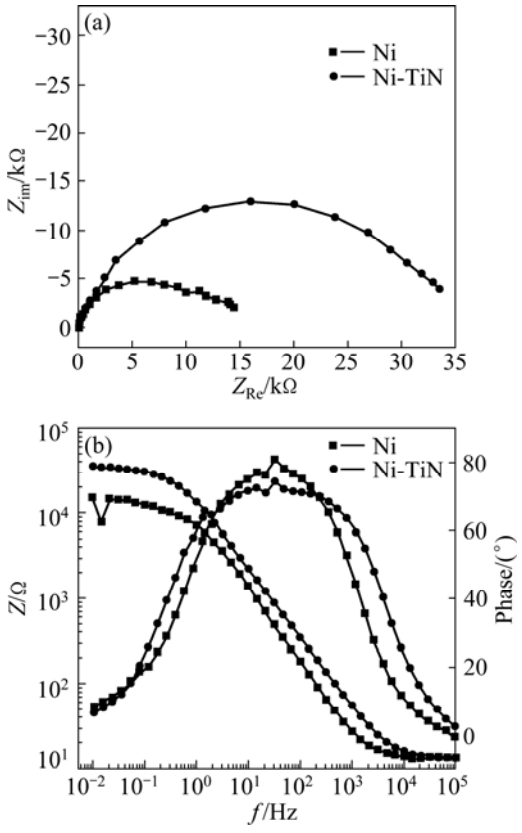

Fig. 8 Nyquist plot (a) and Bode diagram (b) of pure Ni film and Ni-TiN nanocomposite film immersed in 3.5% NaCl solution for 1 h

Table 2 Fitted EIS parameters for pure Ni coating and Ni-TiN composite film in NaCl solution

Film	R_s/(Ω·cm^2)	CPE1-T/(μF·cm^{-2})	CPE1-P	R_1/(Ω·cm^2)	R_t/(Ω·cm^2)	CPE2-T/(μF·cm^{-2})	CPE2-P
Ni	13.12	16.4	0.91	9 841	6535	237	0.65
Ni-TiN	11.25	13.2	0.91	17 685	29 856	131	0.5

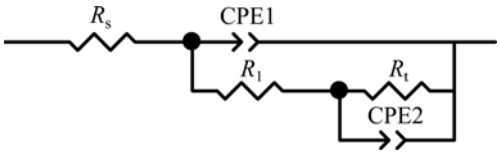

Fig. 9 Equivalent circuit for EIS of pure Ni and Ni-TiN composite films in NaCl solution

seen that the both R_t and R_1 of pure nickel film are much smaller than those of the Ni-TiN nanocomposite film, which means the corrosion rate of the pure nickel film is larger, and the Ni-TiN nanocomposite film possesses good corrosion resistance. Meanwhile, the lower double-layer capacitance value for Ni-TiN nanocomposite film indicates that the surface of Ni coating exposed to corrosion medium is much higher than that of Ni-TiN nanocomposite film [21]. Figure 10 shows the potentiodynamic scanning curves of pure Ni film and Ni-TiN nanocomposite film immersed in 3.5% NaCl solution, from which the corresponding corrosion currents are 2.864×10^{-6} A/cm^2 and 2.739×10^{-7} A/cm^2, respectively. It also indicates that the Ni-TiN nanocomposite film is more resistant to corrosion than the pure Ni coating.

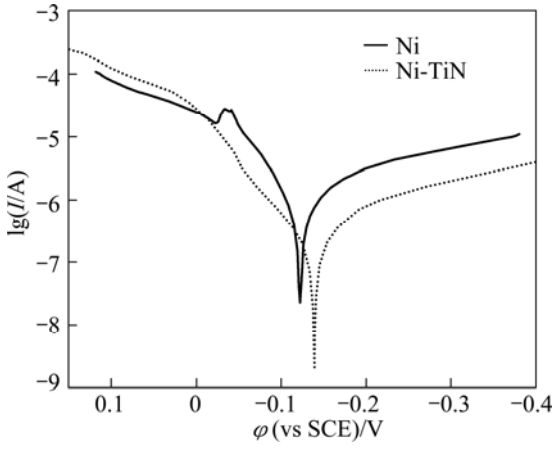

Fig. 10 Potentiodynamic scanning curves of pure Ni film and Ni-TiN nanocomposite film immersed in 3.5% NaCl solution (Scanning rate: 1 mV/s)

4 Conclusions

1) The influences of principal technological parameters including solution agitation speed, TiN nanoparticle concentration, current density, bath temperature and bath pH value on the microstructure of electrodeposited Ni-TiN composite film were investigated and optimized.

2) The optimized Ni-TiN composite film is composed of nickel grains with the average grain size of 50 nm, and TiN nanoparticles distribute uniformly in the Ni-TiN composite film.

3) Ni-TiN nanocomposite film is more resistant to corrosion in 3.5% NaCl solution than pure nickel film.

References

[1] PODLAHA E J. Selective electrodeposition of nanoparticulates into metal matrices [J]. Nano Letters, 2001, 1(8): 413−416.

[2] STAN V, MARITZA G J V H, PAVLA K, JAN P. Different approaches to superhard coatings and nanocomposites [J]. Thin Solid Films, 2005, 476: 1−29.

[3] XU B S, WANG H D, DONG S Y, JIANG B, TU W Y. Electrodeposition nickel silica nano-composites coatings[J]. Electrochemistry Communications, 2005, 7: 572−575.

[4] BENEA L, BONORA P L, BORELLO A, MARTELLI S, WENGER F, PONTHIAUX P, GALLAND J. Composite electrodeposition to obtain nanostructured coatings [J]. J Electrochem Soc, 2001, 148(7): C461−C465.

[5] BENEA L, BONORA P L, BORELLO A, MARTELLI S, WENGER F, PONTHIAUX P, GALLAND J. Preparation and investigation of nanostructured SiC-nickel layers by electrodeposition [J]. Solid State Ionics, 2002, 151: 89−95.

[6] ZHANG Wen-feng, ZHENG Xiao-hu. Microstructure and morphology of worn surface of Ni-ZrO_2 nano-composite electroformings [J]. Surface Technology, 2010, 39(4): 21−24. (in Chinese)

[7] YU Jie, LIU Jian-ping, ZHAO Guo-peng, HU Cheng-gang, ZENG Zhen-ou. Pyro-oxidation resistance of Ni-SiC nano-composite coating [J]. Surface Technology, 2004, 33(6): 31−33. (in Chinese)

[8] LIN C S, HUANG K C. Codeposition and microstructure of nickel-SiC composite coating electrodeposited from sulphamate bath [J]. J Appl Electrochem, 2004, 34: 1013−1019.

[9] TJONG S C, CHEN H. Nanocrystalline materials and coatings [J]. Materials Science & Engineering R, 2004, 45: 1−88.

[10] HOU K H, GER M D, WANG L M, KE S T. The wear behaviour of electro-codeposited Ni-SiC composites [J]. Wear, 2002, 253: 994−1003.

[11] MA C B, CAO F H, ZHANG Z, ZHANG J Q. Electrodeposition of amorphous Ni-P coatings onto Nd-Fe-B permanent magnet substrates [J]. Appl Surf Sci, 2006, 253: 2251−2256.

[12] NWOKO V O, SHREIR L L. Electron micrographic examination of electrodeposited dispersion-hardened nickel [J]. J Appl Electrochem, 1973, 3: 137−141.

[13] GUGLIELMI N. Kinetics of deposition of inert particles from electrolytic baths [J]. J Electrochem Soc, 1972, 119(8): 1009−1012.

[14] NIU Zhao-xia, CAO Fa-he, WANG Wei, ZHANG Zhao, ZHANG Jian-qing, CAO Chu-nan. Electrodeposition of Ni-SiC nanocomposite film [J]. Transactions of Nonferrous Metals Society of China, 2007, 17(1): 9−15.

[15] CAI C, ZHU X B, ZHENG G Q, YUAN Y N, HUANG X Q, CAO F H, YANG J F, ZHANG Z. Electrodeposition and characterization of nano-structured Ni-SiC composite films [J]. Surf Coat Technol, 2011, 205: 3448−3454.

[16] WALTER E C, ZACH M P, FAVIER F, MURRAY B J, INAZU K, HEMMINGER J C, PENNER R M. Metal nanowire arrays by electrodeposition [J]. Chem Phys Chem, 2003, 4: 131−138.

[17] NOWAK P, SOCHA R P, KAISHEVA M, FRANSAER J, CELIS J P, STOINOV Z. Electrochemical investigation of the codeposition of SiC and SiO_2 particles with nickel [J]. J Appl Electrochem, 2000, 30: 429−437.

[18] TSAY P, HU C C. Non-anomalous codeposition of iron-nickel alloys using pulse-reverse electroplating through means of experimental strategies [J]. J Electrochem Soc C, 2002, 149: 492−497.

[19] van der WEIJDE D H, van WESTING E P M, de WIT J H W. Electrochemical techniques for delamination studies [J]. Corros Sci, 1995, 36(4): 643−652.

[20] CAMPESTRINI P, van WESTING E P M, de WIT J H W. Influence of surface preparation on performance of chromate conversion coating on alclad 2024 aluminum alloy – Part II. EIS investigation [J]. Electrochim Acta, 2001, 46: 2631−2647.

[21] ARUNA S T, BINDU C N, EZHIL SELVI V, WILLIAM GRIPS V K, RAJAM K S. Synthesis and properties of electrodeposited Ni/ceria nanocomposite coatings [J]. Surf Coat Technol, 2006, 200: 6871−6880.

纳米结构 Ni-TiN 复合薄膜的电沉积及腐蚀行为

朱旭蓓[1], 蔡 超[2,3], 郑国渠[1], 张 昭[3], 李劲风[4]

1. 浙江工业大学 化工学院，杭州 310014；
2. 西安交通大学 材料强度国家重点实验室，西安 710049；
3. 浙江大学 化学系，杭州 310027；
4. 中南大学 材料科学与工程学院，长沙 410083

摘 要：采用电沉积方法在黄铜基底上制备纳米结构的 Ni-TiN 复合薄膜。用扫描电镜(SEM)及透射电镜(TEM)对其微观结构进行表征，利用 X 射线衍射(XRD)分析其平均晶粒尺寸，采用极化曲线及电化学阻抗谱(EIS)研究其腐蚀行为。结果表明，电沉积的电流密度、TiN 纳米粒子的浓度、搅拌速度、溶液温度及 pH 值对电沉积薄膜形貌的影响较大。制备的 Ni-TiNi 电沉积薄膜的平均晶粒尺寸约为 50 nm。纳米结构的 Ni-TiNi 电沉积薄膜的耐腐蚀性能远优于纯 Ni 沉积薄膜的。

关键词：Ni-TiN 纳米复合薄膜；电沉积；电化学阻抗谱

(Edited by YANG Hua)